Electric-dipole transitions and octupole softness in odd-A rare-earth nuclei

G. B. Hagemann
The Niels Bohr Institute, University of Copenhagen, Tandem Accelerator Laboratory, DK 4000 Roskilde, Denmark

I. Hamamoto and W. Satuła*
Department of Mathematical Physics, University of Lund, Box 118, S-221 00 Lund, Sweden
(Received 23 July 1992)

It is found that $B(E1)$ values calculated by using a model in which one quasiparticle is coupled to a rotor are more than an order of magnitude too small compared with measured $B(E1)$ values in low-energy transitions observed in the yrast spectroscopy of odd-A rare-earth nuclei. Thus, the measured $B(E1)$ values are analyzed by introducing the parameters which effectively take into account the octupole softness. The parameters thus determined for two sets of bands in ^{169}Lu are considerably different. Interpreting the difference in terms of a difference in blocking of the particular orbitals in octupole vibration amplitudes, an estimate of the difference is made using a microscopic model. A full agreement between the estimated values and the values necessary for reproducing data is not obtained.

PACS number(s): 21.10.Ky, 23.20.−g, 21.60.Cs

I. INTRODUCTION

Low-energy electric-dipole ($E1$) transitions observed in nuclei are often strongly hindered (see, for example, Ref. [1]). The observation of $E1$ decay modes in competition with stretched electric-quadrupole ($E2$) transitions with the present day experimental techniques means that the $B(E1)$ values have to be of the order of or larger than $10^{-4}\ e^2\,\mathrm{fm}^2$. That means, the hindrance factor for measured $B(E1)$ values has to be of the order of or weaker than 10^{-4} as compared with the single-particle estimate (Weisskopf unit).

The octupole softness (or deformation) together with quadrupole deformation leads to an enhanced dipole moment, which was estimated already in the 1950's by Strutinsky [2] and by Bohr and Mottelson [3]. It has been recognized that relatively strong $E1$ transitions (though much weaker than the Weisskopf unit) are observed in nuclei which are supposed to be soft against octupole deformation. There are experimental indications (for example, low-lying negative-parity states in even-even nuclei [4]) that some nuclei in the Ba-Sm and the Ra-Th region are unstable against octupole deformation. Theoretical calculations (Refs. [5,6]; for more recent works, see Refs. [7–9] and references quoted therein) also indicate that the nuclear shape of these nuclei in the body-fixed frame is unstable with respect to octupole deformation, though in the available publications only the axially symmetric octupole deformation has been explored for the ground states. In the present paper we study low-energy $E1$ transitions observed in the yrast spectroscopy of quadrupole-deformed odd-A rare-earth nuclei, which are usually supposed to be stable against octupole deformations (for example, see Ref. [10]) and in which no strongly collective octupole vibrational states are observed.

In order to make a reliable estimate of the $E1$ strengths of low-energy transitions, it is essential to use reasonable values of $E1$ effective charge, to include a sufficiently large space of one-particle orbitals, to carefully include the pair-correlation effect, and to take into account all important matrix elements of the Coriolis coupling [11]. Already in the middle of the 1960's the $E1$ transitions in well-deformed rare-earth nuclei were estimated in several publications (see, for example, Refs. [12–14]). Though experimental data were well reproduced in some of those publications, all the essential elements mentioned above are not satisfied in any of those calculations. Thus, the understanding of the physics based on those calculations can be questioned. Moreover, the recent high-spin yrast spectroscopy provides information on the angular momentum dependence of the $E1$ transition strengths in a wide range of angular momentum. The angular momentum dependence was not available in the 1960's except for the data [15] on ^{177}Hf. The observed angular momentum dependence does not follow the Alaga rule (see, for example, Ref. [16]),

$$B(E1{:}K_i,I_i\rightarrow K_f,I_f) = [\langle I_iK_i1\nu|I_fK_f\rangle M(E1,\nu=K_f-K_i)]^2 .$$

The Alaga rule is expected to work when the wave functions of axially symmetric shape are not seriously disturbed by rotational perturbation and when the transition matrix elements are governed by the main component of the wave functions. When the Coriolis perturbation becomes appreciable, the three types of $E1$ transitions, $I\rightarrow I-1$, $I\rightarrow I$, $I\rightarrow I+1$, between a given pair of rotational bands should be regarded as different types of transitions [17], providing independent information on the

*On leave of absence from Institute of Theoretical Physics, University of Warsaw, Poland.

relative structure of the wave functions of the initial and the final states. It is noted that in the Alage rule the $E1$ matrix elements of the above three types of transitions are related by Clebsch-Gordan coefficients since the intrinsic $E1$ matrix elements, $M(E1,\nu=K_f-K_i)$, are common in those three transitions.

In Sec. II A the hindrance mechanism of low-energy $E1$ transitions is examined in detail. In Sec. II B, using the model (see Ref. [11]) of one quasiparticle coupled to a rotor with a sufficiently large single-particle space, we first try to reproduce as well as possible the observed level scheme in the angular momentum region before the lowest band crossing. Then, using the resulting wave functions we estimate the $E1$ transition strengths employing the $E1$ effective charges as suggested in Ref. [1]. The obtained $B(E1)$ values turn out to be too small as compared with experimental data. Thus, in Sec. III A the available experimental data on $E1$ transitions are analyzed by introducing the parameters b_ν, which effectively take into account the contributions from octupole softness to the $E1$ transition strengths [11]. For completeness, the analysis of experimental data on ^{177}Hf and ^{169}Lu, which is taken from Refs. [11] and [18], respectively, is also included in the present paper. In Sec. III B we investigate whether the magnitudes of the obtained b_ν parameters can be reasonably well understood in terms of a microscopic model. The summary is presented in Sec. IV.

II. ESTIMATE OF $E1$ TRANSITION STRENGTH WITHOUT INVOKING OCTUPOLE SOFTNESS

A. Hindrance mechanism for low-energy $E1$ transitions

The reason for the hindrance of low-energy $E1$ transitions is many fold: (a) The $E1$ transition operator has to be orthogonal to the excitation of the center-of-mass motion. (b) The major part of the $E1$ strength lying originally in the low-energy region is shifted to the region of higher energy, because of the repulsive character of the isospin-dependent part of the nuclear residual interaction. This interaction is responsible for pushing up the energy of the giant dipole resonance (GDR) from the excitation energy of $1\hbar\omega_0$. (c) Due to the nuclear shell structure, the $rY_{1\nu}$ matrix elements between Nilsson orbitals closely lying at the deformation of the ground states are usually strongly hindered. (d) The pairing factor for electric transitions without changing the number of quasiparticles is $(uu-vv)^2$, which could be much smaller than unity.

The reduction factor coming from (a) and (b) may be expressed in the form of an effective charge of $E1$ transitions, which is considerably smaller than unity. The expression, which can be found in Eq. (6-330) on p. 448 of Ref. [1], is

$$e_{\rm eff}(E1)=-\frac{1}{2}e\left[\tau_z-\frac{N-Z}{A}\right](1+\chi)\ , \tag{1}$$

where χ is the polarizability due to GDR. Assuming that the excitation energy of the GDR is much larger than the $E1$ transition energy considered, one can estimate [1] $\chi\approx-0.7$, and the expression (1) provides, for example, for the nucleus ^{177}Hf

$$e_{\rm eff}(E1)=\begin{cases}-0.12e & \text{for neutrons,}\\ +0.18e & \text{for protons .}\end{cases} \tag{2}$$

Thus, the effective charge (2) leads to a reduction of $B(E1)$ values by a factor of 1.44×10^{-2} for neutrons and 3.24×10^{-2} for protons, respectively. The possible dependence of the effective charge on rotational frequency is neglected in the following, since the investigation in Ref. [19], using a simple model, shows that the dependence is weak and is almost negligible in the low-rotational-frequency region relevant to the present investigation.

In Table I we tabulated numerical values of calculated matrix elements $\langle rY_{1\nu}\rangle$ for the pairs of orbitals which are relevant to the presently investigated low-energy $E1$ transitions. Calculated matrix elements $\langle r^3Y_{3\nu}\rangle$ are also shown for reference. One-particle orbitals are designated by the asymptotic quantum numbers. For comparison, we show some examples of the calculated matrix elements marked by an asterisk, which are allowed by the difference of the asymptotic quantum numbers. The one-particle energy difference of pairs of this latter type is, for example, about equal to $\hbar\omega_z=\hbar\omega_0(1-\frac{2}{3}\varepsilon)\approx0.8\hbar\omega_0\approx6$ MeV in the case of the operator rY_{10}. Except for a "relatively large" rY_{10} matrix element estimated for the pair of the orbitals, [541 $\frac{1}{2}$] and [411 $\frac{1}{2}$], in which an appreciable amount of the admixed asymptotic [521 $\frac{1}{2}$] component in the calculated [541 $\frac{1}{2}$] orbital contributes to the rY_{10} matrix element, the estimated $rY_{1\nu}$ matrix elements between closely lying one-particle orbitals are very small. They are less than a few percent of those between a pair of orbitals for which the change of the asymptotic quantum numbers allows the $E1$ transitions. That means the hindrance of the $rY_{1\nu}$ matrix elements due to the nuclear shell structure gives rise to a reduction factor of $B(E1)$ values which is appreciably stronger than 10^{-2}.

In Fig. 1 the reduction factor coming from (d) is exhibited for the relevant pairs of orbitals in various nuclei investigated in the present work. The reduction factor depends sensitively on the positions of the pair of orbital relative to the Fermi level. It is seen from Fig. 1 that the pair-correlation factor $(uu-vv)^2$ gives rise to a reduction factor of at least 0.1 in the relevant $B(E1)$ values, but the reduction may become much stronger depending on nuclei and configurations.

B. Calculation of $E1$ strength

The model described in Ref. [11] is employed in the present work. Namely, using the stretched coordinates we solve the one-particle motion in a quadrupole-deformed modified harmonic oscillator (MHO) potential. Then, including the pair correlation in the BCS approximation, we diagonalize the Hamiltonian in which one quasiparticle is coupled to an axially symmetric rotor. In the diagonalization all the one-quasiparticle orbits in a given stretched oscillator shell N_t are included. Pair-gap

TABLE I. Calculated matrix elements between one-particle orbitals in the MHO potential. A few pairs of orbitals (marked by an asterisk), between which the matrix elements $\langle rY_{1\nu}\rangle$ are allowed by asymptotic quantum numbers, are also chosen for reference. The calculated energy difference of the one-particle orbitals, $|\Delta\varepsilon|$, is given in units of $\hbar\omega_0$. Parameters used are $A=169$ and $Z=71$ with ε, κ, and μ given in the table.

Nilsson states $[Nn_z\Lambda\Omega]$		$\lvert\Delta\varepsilon\rvert$ ($\hbar\omega_0$)	$\langle rY_{10}\rangle$ (fm)	$\langle rY_{1\pm1}\rangle$ (fm)	$\langle r^3Y_{30}\rangle$ (fm^3)	$\langle r^3Y_{3\pm1}\rangle$ (fm^3)
		Protons: $\varepsilon=0.27$, $\kappa=0.0637$, $\mu=0.60$				
$[523\ \frac{7}{2}]$	$[404\ \frac{7}{2}]$	0.143	0.014		−9.6	
$[514\ \frac{9}{2}]$	$[404\ \frac{7}{2}]$	0.076		0.024		−11.8
$[541\ \frac{1}{2}]$	$[411\ \frac{1}{2}]$	0.262	0.095	0.020	−35.9	−10.3
$[541\ \frac{1}{2}]$	$[660\ \frac{1}{2}]$	0.064	0.058	0.045	−25.4	−32.1
*$[532\ \frac{5}{2}]$	$[431\ \frac{3}{2}]$*	0.846		1.211		66.9
*$[532\ \frac{5}{2}]$	$[422\ \frac{5}{2}]$*	0.684	1.486		18.5	
*$[521\ \frac{1}{2}]$	$[411\ \frac{1}{2}]$*	0.963	1.360	0.122	1.2	−0.2
		Neutrons: $\varepsilon=0.27$, $\kappa=0.0637$, $\mu=0.42$				
$[521\ \frac{3}{2}]$	$[642\ \frac{5}{2}]$	0.017		0.040		−41.0
$[523\ \frac{5}{2}]$	$[642\ \frac{5}{2}]$	0.054	0.032		−23.3	
$[514\ \frac{7}{2}]$	$[624\ \frac{9}{2}]$	0.034		0.030		−17.6
*$[532\ \frac{5}{2}]$	$[642\ \frac{5}{2}]$*	0.712	1.620		38.3	
*$[541\ \frac{3}{2}]$	$[642\ \frac{5}{2}]$*	0.857		1.170		74.5

parameters Δ are taken from the measured odd-even mass difference [20]. By varying quadrupole deformation parameters ε, moments of inertia J, and Coriolis reduction factors ξ within acceptable ranges, we try to reproduce the relevant level schemes as well as possible. Parameters fixed in this way are given in Table II. In the present calculation the measured bandhead energy is identified with the energy of the given angular momentum state obtained from the particle-rotor calculation. Using the resulting wave functions, the $E1$ transition matrix elements are calculated.

Squares in Fig. 2 show the calculated $B(E1)$ values in ^{177}Hf, in which experimental data are available for three types of $E1$ transitions (i.e., for $I_f>I_i$, $I_f=I_i$, and $I_f<I_i$). As the values of the neutron and proton $E1$ effective charges, in the present work we use $-0.15e$ and $+0.20e$, which are the values obtained from the analysis of experimental data on the nuclei around ^{208}Pb [21]. The absolute magnitudes of the effective charges used in our calculations are even somewhat larger than the values obtained from the expression (1). From Fig. 2 it is seen that the calculated $B(E1)$ values are always much smaller than $10^{-4}\ e^2\,\mathrm{fm}^2$ and, thus, much smaller than observed values. Noticing that the final states belong to the band $[514\ \frac{7}{2}]$, while the initial states belong to the band $[624\ \frac{9}{2}]$, the dependence of the (open and filled) squares in Fig. 2 on the sign of the variable, $I_f(I_f+1)-I_i(I_i+1)$ can be understood in terms of angular momentum alignment due to the rotational perturbation. Namely, the odd neutron in the $[624\ \frac{9}{2}]$ band, which occupies in essence $i_{13/2}$ orbitals, aligns its angular momentum already under a small rotation, while the one in $[514\ \frac{7}{2}]$ band does little. Consequently, the $E1$ transitions with the angular momentum change $I^+\rightarrow(I-1)^-$ are most favorable [i.e., the $B(E1)$ values are the largest], while those with $I^+\rightarrow(I+1)^-$ are most unfavorable. The effect of the alignment differences in the initial and the final state on the three types of the $E1$ matrix elements ($I\rightarrow1$ and $I\rightarrow I\pm1$) can be seen from the relative magnitudes of squares in Fig. 2 and is in agreement with the result of the calculations using the cranking model [17]. However, the dependence of the magnitudes of those calculated $B(E1)$ values on the sign of the variable $I_f(I_f+1)-I_i(I_i+1)$ is clearly in disagreement with experimental data. See Fig. 7.

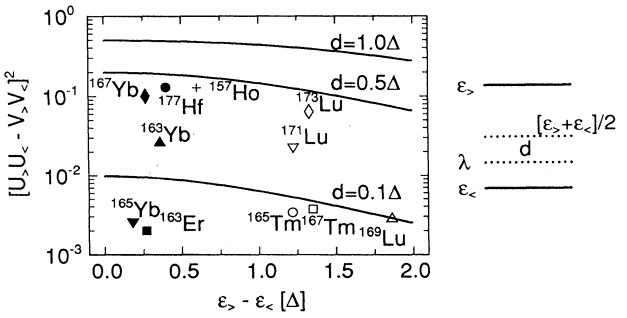

FIG. 1. Calculated pairing factor $(uu-vv)^2$ for the pairs of orbitals in the nuclei investigated. The value plotted for the nucleus ^{169}Lu is for the pair $[411\ \frac{1}{2}]$ and $[541\ \frac{1}{2}]$. Three additional lines are plotted, which are calculated for three different positions of the pair of the orbitals relative to the Fermi level λ, since the pairing factor is very sensitive to the relative position.

TABLE II. Parameters used in numerical calculations: quadrupole deformation ε, neutron (proton) pairing gap in odd-N (odd-Z) nuclei Δ, moment of inertia J, and Coriolis attenuation factor ξ. In order to reproduce the experimental spectra in Tm and Lu nuclei we had to change the Nilsson spectrum before the particle-rotor calculations. For Tm nuclei we shifted first the energy of the $N_t=5$ shell by $-0.07\hbar\omega_0$ ($-0.06\hbar\omega_0$) for ^{165}Tm (^{167}Tm). In the next step the energies of the [411 $\frac{1}{2}$], [541 $\frac{1}{2}$], and [523 $\frac{7}{2}$] orbitals were shifted by $-0.14\hbar\omega_0$, $-0.06\hbar\omega_0$, and $0.14\hbar\omega_0(0.13\hbar\omega_0)$ for ^{165}Tm (^{167}Tm), respectively. For Lu nuclei we shifted the energy of the [411 $\frac{1}{2}$] and [541 $\frac{1}{2}$] orbitals by $-0.14\hbar\omega_0$ and $-0.05\hbar\omega_0$ in ^{169}Lu, by $-0.14\hbar\omega_0$ and $-0.07\hbar\omega_0$ in ^{171}Lu, and by $-0.15\hbar\omega_0$ and $-0.08\hbar\omega_0$ in ^{173}Lu, respectively.

Nucleus	$[Nn_z\Lambda\Omega]^i\rightarrow[Nn_z\Lambda\Omega]^{(f)}$	ε	Δ (MeV)	$\hbar^2/2J$ (MeV)	ξ
$^{157}_{67}Ho_{90}$	[404 $\frac{7}{2}$]→[523 $\frac{7}{2}$]	0.220	1.20	0.0168	0.70
$^{165}_{69}Tm_{96}$	[411 $\frac{1}{2}$]→[541 $\frac{1}{2}$]	0.275	1.00	0.013	0.70
$^{167}_{69}Tm_{98}$	[411 $\frac{1}{2}$]→[541 $\frac{1}{2}$]	0.275	0.95	0.018	0.70
$^{169}_{71}Lu_{98}$	[411 $\frac{1}{2}$]→[541 $\frac{1}{2}$]	0.270	1.00	0.014	0.70
	[514 $\frac{9}{2}$]→[404 $\frac{7}{2}$]	0.270	1.00	0.014	0.70
$^{171}_{71}Lu_{100}$	[411 $\frac{1}{2}$]→[541 $\frac{1}{2}$]	0.275	0.98	0.0128	0.80
$^{173}_{71}Lu_{102}$	[411 $\frac{1}{2}$]→[541 $\frac{1}{2}$]	0.275	0.95	0.0125	0.90
$^{163}_{68}Er_{95}$	[523 $\frac{5}{2}$]→[642 $\frac{5}{2}$]	0.250	1.05	0.012	0.65
$^{163}_{70}Yb_{93}$	[521 $\frac{3}{2}$]→[642 $\frac{5}{2}$]	0.230	1.05	0.014	0.65
$^{165}_{70}Yb_{95}$	[523 $\frac{5}{2}$]→[642 $\frac{5}{2}$]	0.240	1.15	0.0128	0.65
$^{167}_{70}Yb_{97}$	[523 $\frac{5}{2}$]→[642 $\frac{5}{2}$]	0.250	1.05	0.0115	0.65
$^{177}_{72}Hf_{105}$	[624 $\frac{9}{2}$]→[514 $\frac{7}{2}$]	0.265	0.70	0.014	0.80

III. ANALYSIS OF $E1$ TRANSITION STRENGTHS INCLUDING OCTUPOLE SOFTNESS

A. Analysis of experimental data in terms of octupole softness parameters

Since it is impossible to obtain measured magnitudes of $B(E1)$ values in the model calculations presented in the previous section, in the present section we first analyze available experimental $B(E1)$ values in terms of parameters, which effectively express the effect of octupole vibrations on $E1$ transitions. In Ref. [14] the importance of taking into account the effect of octupole vibration with $K^\pi=0^-$ in the estimate of $E1$ transitions in ^{177}Hf was stressed.

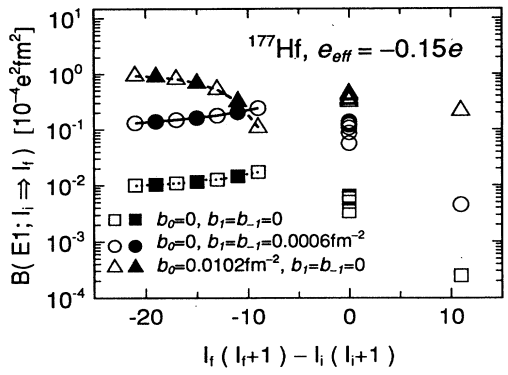

FIG. 2. Calculated $B(E1)$ values from the [624 $\frac{9}{2}$] to the [514 $\frac{7}{2}$] band in ^{177}Hf. Squares, circles, and triangles express the results without including b_ν parameters, with b_1 parameter only, and with b_0 parameter only. $B(E1)$ values calculated, including both b_0 and b_1, are shown in Fig. 7 in comparison with experimental values.

Following the analysis in Ref. [11], we write the $E1$ transition operator as

$$\mathcal{O}(E1,\mu)=\sum_\nu \mathcal{O}(E1,\nu)D^1_{\mu\nu} , \tag{3}$$

where the $E1$ transition operator in the intrinsic coordinate system is expressed as

$$\mathcal{O}(E1,\nu)=e_{\rm eff}(E1)rY_{1\nu}+eb_\nu r^3Y_{3\nu} . \tag{4}$$

The expression of the parameters b_ν is written as

$$eb_\nu=\sum_{i,\tau}x_3(\tau)\left[\frac{-2}{\hbar\omega_i}\right]\langle i,\tau|r^3Y^*_{3\nu}|0\rangle \times\langle 0|\tilde{\mathcal{O}}(E1,\nu)|i,\tau\rangle,\quad x_3(\tau)=\kappa_0+\tau\kappa_1 , \tag{5}$$

where

$$\tilde{\mathcal{O}}(E1,\nu)=e_{\rm eff}(E1)rY_{1\nu} \tag{6}$$

and $|i\rangle$ expresses all possible $K^\pi=0^-$ (or 1^-) random phase approximation (RPA) excitation modes, $\tau=\pm1$ for like (unlike) particles, and κ_0 (κ_1) denotes the isoscalar (isovector) coupling constant for the bare octupole-octupole interaction. The expression (4) was derived assuming that the particle octupole-vibration coupling can be treated in perturbation. The contribution to the $E1$ operator [$\mathcal{O}(E1,\nu)$] coming from the octupole vibrations in quadrupole-deformed nuclei is represented by the second term in Eq. (4). In the intrinsic system of the deformed nuclei the particle-vibration coupling is written as $x_3(\tau)r^3Y_{3\nu}r^3Y^*_{3\nu}$, without having the sum over the quantum number ν. Namely, the one-particle operator $r^3Y_{3\nu}$ appearing on the right-hand side (rhs) of Eq. (4) comes

TABLE III. Values of the parameters b_0 and b_1 needed to reproduce experimental $B(E1)$ values. The quality of the reproduction for respective transitions is seen in Figs. 3–7. The values of b_ν, which we feel are determined in a relatively reliable way, are shown without parentheses.

Nucleus	$[Nn_z\Lambda\Omega]^{(i)}\rightarrow[Nn_z\Lambda\Omega]^{(f)}$	e_{eff}	b_0 (fm^{-2})	b_1 (fm^{-2})
$^{157}_{67}Ho_{90}$	$[404\ \frac{7}{2}]\rightarrow[523\ \frac{7}{2}]$	$0.2e$	(0.02)	(0.0)
$^{165}_{69}Tm_{96}$	$[411\ \frac{1}{2}]\rightarrow[541\ \frac{1}{2}]$	$0.2e$	-0.0054	0.018
$^{167}_{69}Tm_{98}$	$[411\ \frac{1}{2}]\rightarrow[541\ \frac{1}{2}]$	$0.2e$	(0.025)	(0.0)
$^{169}_{71}Lu_{98}$	$[411\ \frac{1}{2}]\rightarrow[541\ \frac{1}{2}]$	$0.2e$	-0.0039	0.013
	$[514\ \frac{9}{2}]\rightarrow[404\ \frac{7}{2}]$	$0.2e$	0.01	0.01
$^{171}_{71}Lu_{100}$	$[411\ \frac{1}{2}]\rightarrow[541\ \frac{1}{2}]$	$0.2e$	(0.00176)	(0.022)
$^{173}_{71}Lu_{102}$	$[411\ \frac{1}{2}]\rightarrow[541\ \frac{1}{2}]$	$0.2e$	(0.0)	(0.010)
$^{163}_{68}Er_{95}$	$[523\ \frac{5}{2}]\rightarrow[642\ \frac{5}{2}]$	$-0.15e$	(0.0112)	(-0.0014)
$^{163}_{70}Yb_{93}$	$[521\ \frac{3}{2}]\rightarrow[642\ \frac{5}{2}]$	$-0.15e$	(0.01)	(10^{-6})
$^{165}_{70}Yb_{95}$	$[523\ \frac{5}{2}]\rightarrow[642\ \frac{5}{2}]$	$-0.15e$	(0.0112)	(-10^{-6})
$^{167}_{70}Yb_{97}$	$[523\ \frac{5}{2}]\rightarrow[642\ \frac{5}{2}]$	$-0.15e$	(0.006)	(10^{-6})
$^{177}_{72}Hf_{105}$	$[624\ \frac{9}{2}]\rightarrow[514\ \frac{7}{2}]$	$-0.15e$	0.0102	0.0006

from the particle part of the particle-vibration coupling and does not represent the tensorial character of the total expression. Since both terms on the rhs of Eq. (4) are dipole operators in the intrinsic system, the transformation to the laboratory system is performed using D^1 Wigner functions, as is written in the expression (3). In the following the dependence of b_ν on rotational frequency is neglected.

Using the wave functions obtained in the previous section, we evaluate the matrix elements of the $E1$ transition operator (4) and determine the values of b_0 and $b_{\pm1}$ ($b_1=b_{-1}$) which are necessary for reproducing the observed $B(E1)$ values. The resulting b_ν parameters are given in Table III, while, in Figs. 3–7, the calculated $B(E1)$ values are compared with experimental values. The experimental values which we adopted are given in Table IV. Supposing that the experimental $B(E1)$ values adopted are quite reliable, we feel comfortable at the quality of the reproduction of the observed $B(E1)$ values only for $E1$ transitions in the nuclei ^{165}Tm, ^{169}Lu, and ^{177}Hf, for which the data impose the largest limitations on the mutual combinations of b_0 and b_1. These resulting b_ν parameters can be quantitatively used in later discussions. Thus, the b_ν values determined for other nuclei are given within parentheses in Table III. Generally speaking, the accuracy of $B(E1)$ values estimated from experimental information is not very high, and the limit of the ambiguity involved in the estimate is difficult to evaluate precisely. In almost all cases there is no lifetime measurement and, thus, $B(E1)$ values were estimated from the measured branching ratios $B(E1)/B(E2)$,

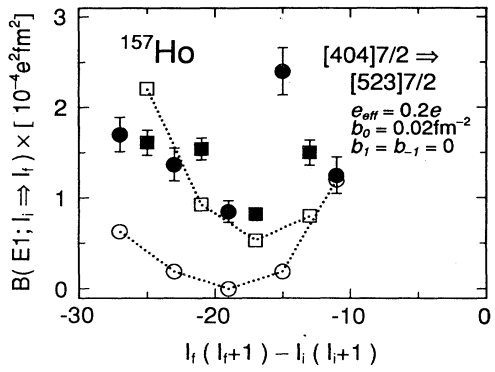

FIG. 3. Comparison between experimental and calculated $B(E1)$ values for ^{157}Ho. The filled (open) symbols denote the experimental (calculated) values. The circles (squares) are used for transitions with different signature α combinations I^i $[\alpha=\frac{1}{2}\ (-\frac{1}{2})]\rightarrow I^f$ $[\alpha=-\frac{1}{2}\ (\frac{1}{2})]$, respectively. The dotted line connecting the calculated $B(E1)$ values shows the signature dependence obtained in the calculations. The same convention for the symbols (lines) is used in Figs. 3–7. Moreover, the transitions $I\rightarrow I$ are marked by triangles. The discrepancy between the calculated and experimental $B(E1)$ values comes, presumably, from the quadrupole softness [30] which is not taken into account in our calculations. In the case of complete overlap between theory and experiment the theoretical (open) symbol is hidden throughout Figs. 4–7.

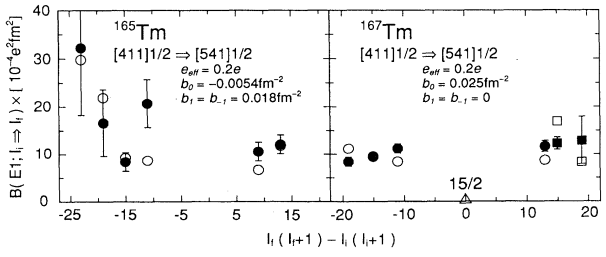

FIG. 4. Comparison between experimental and calculated $B(E1)$ values for ^{165}Tm and ^{167}Tm. The calculated $B(E1)$ value of the transition from $\frac{15}{2}^+$ to $\frac{15}{2}^-$ in ^{167}Tm is shown for reference. The b_ν parameters in ^{167}Tm turn out to be not uniquely determined. The comparable agreement between theory and experiment was obtained using, for example, $b_0=-0.004$ fm^{-2} and $b_1=0.013$ fm^{-2}.

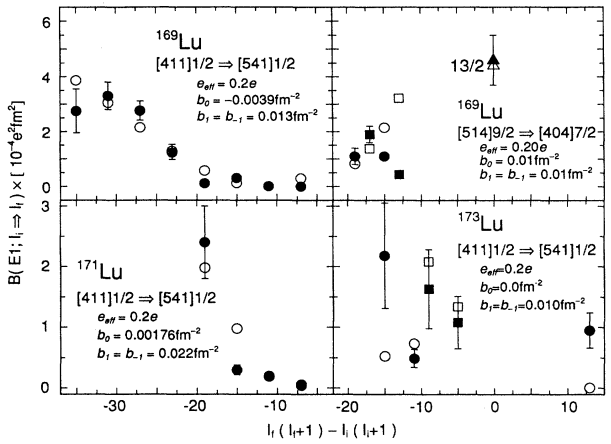

FIG. 5. Comparison between experimental and calculated $B(E1)$ values for ^{169,171,173}Lu. The agreement between experiment and theory seems to be satisfactorily good for ^{169}Lu and ^{171}Lu and rather poor for ^{173}Lu. However, in ^{171}Lu the sudden increase of $B(E1)$ value for the $\frac{19}{2}^+ \rightarrow \frac{17}{2}^-$ transition can cause a large ambiguity in the determination of the b_ν parameters. For ^{171}Lu and ^{173}Lu we performed also the calculations using the Nilsson spectrum similar to the one used for Tm nuclei (see caption to Table II). The resulting b_ν parameters appeared to be very close in both versions of our calculations.

while the $B(E2)$ values of the stretched $E2$ transitions were evaluated assuming reasonable values of the intrinsic quadrupole moment.

In spite of the presence of the ambiguities mentioned above it may be concluded that (see Table III) (i) the values of b_0 and/or b_1 of the order of 10^{-2} fm^2 are necessary for reproducing experimental data, and (ii) the obtained b_ν values depend on nuclei and are sensitive to a selected pair of bands.

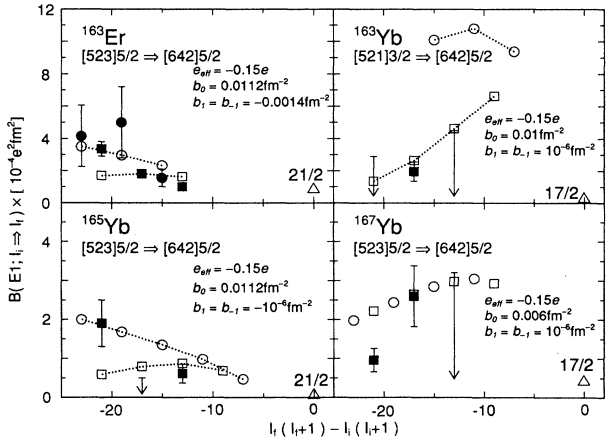

FIG. 6. Comparison between experimental and calculated $B(E1)$ values for ^{163}Er and ^{163,165,167}Yb. The calculated $B(E1)$ values of the transition from I^- to I^+ [$I = \frac{21}{2}$ ($\frac{17}{2}$) for ^{163}Er and ^{165}Yb (^{163}Yb and ^{167}Yb)] are shown for reference. Since these transitions are not observed (i.e., are very weak), the theoretical values had to be kept as small as (or smaller than) the plotted values in the figure. Both the agreement between the observed level scheme and the calcualted one as well as the quality of the experimental data are not satisfactory for all nuclei. Thus the obtained b_ν values have rather large ambiguities.

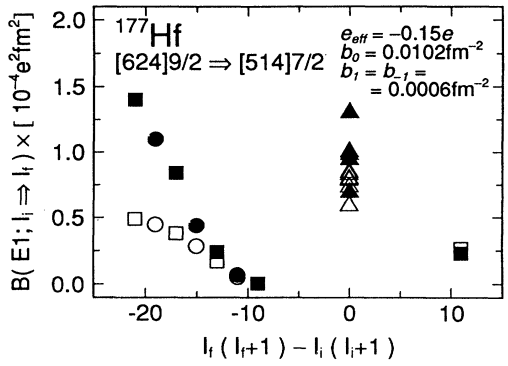

FIG. 7. Comparison between experimental and calculated $B(E1)$ values for ^{177}Hf. The analysis is taken from Ref. [11]. The result of the analysis presented here is slightly different from the one published in Ref. [11], since a minor error in the computer program was here corrected. The agreement between experiment and theory is satisfactory.

For the pair of bands in ^{177}Hf in Fig. 2 we show, for reference, the contributions obtained by including either only b_0 or only b_1. It is seen that in this example the inclusion of the indicated amount of either only b_0 or only b_1 always increases the calculated $B(E1)$ values, and the b_0 or the b_1 parameter produces a clearly different dependence of $B(E1)$ values on the variable $I_f(I_f+i) - I_i(I_i+1)$. Therefore, the determination of the b_ν parameters from comparison with available experimental data may be regarded as being reasonably unique.

B. Estimate of octupole softness parameters based on a microscopic model

A crucial point in the analysis presented in Sec. III A is whether the obtained b_ν parameters can be reasonably well understood in terms of a microscopic model or not. Already, before performing numerical estimates, one sees that a quantitative estimate of the b_ν parameters is very difficult. In the estimate of the expression (5) the RPA model must be free from the excitation of the center-of-mass motion and contain the isoscalar as well as the isovector octupole (and dipole) correlations. The calculated b_ν values depend also very sensitively on the radial distribution of the neutron and proton densities and, thus, on the mutual polarization effect between neutrons and protons. Considering the accuracy of possible theoretical models available at present, we feel that probably nobody can calculate b_ν values in quite a reliable way. Therefore, in the following we give up on obtaining the absolute magnitudes of the b_ν parameters. Instead, we try to examine the difference of b_ν values for various $E1$ transitions. If the even-even core is the same, the difference comes from the blocking effect due to the presence of the odd particle. The blocking effect depends only on the particular orbitals involved in the $E1$ transitions and may

TABLE IV. Experimental $B(E1)$ values adopted in the present work. The $B(E1)$ values are given for the indicated transitions. If the initial and the final state are exchanged in the observed transitions, the $B(E1)$ values are corrected by the corresponding statistical factor and are denoted by an asterisk. All $B(E1)$ values in Tm (see Refs. [23,24]), Lu (see Refs. [18,25]), Er (see Ref. [26]), and Yb (see Refs. [27,28]) were extracted from experimental branching ratios assuming $Q_t^2=50$ b^2. The $B(E1)$ values of the first three transitions in ^{157}Ho (see Ref. [29]) were obtained using $Q_t^2=36$ b^2, while those of the remaining ones using $Q_t^2=16$ b^2. See Ref. [30] for the measured lifetime of ^{157}Ho. The data of ^{177}Hf are taken from the analysis in Tables 4–9 of Ref. [1] (see also [15]). In the second column we show also the difference of the observed bandhead energy ΔE. In the case of ^{165}Tm and ^{165}Yb the bandhead energy of either the initial or the final band is not known.

Nucleus	ΔE (keV)	$[Nn_z\Lambda\Omega]^{(i)}\rightarrow$ $[Nn_z\Lambda\Omega]^{(f)}$	E_γ (keV)	$I^{(i)}$	$I^{(f)}$	$B(E1)$ ($10^{-4}e^2$fm^2)
			Odd proton			
$^{165}_{69}Tm_{96}$		$[411\ \frac{1}{2}]\rightarrow[541\ \frac{1}{2}]$	134.6	$\frac{7}{2}^+$	$\frac{9}{2}^-$	10.6±2*
			120.4	$\frac{11}{2}^+$	$\frac{9}{2}^-$	20.7±5
			84.2	$\frac{11}{2}^+$	$\frac{13}{2}^-$	12.1±2*
			271.1	$\frac{15}{2}^+$	$\frac{13}{2}^-$	8.4±2
			420.0	$\frac{19}{2}^+$	$\frac{17}{2}^-$	16.6±7
			561.8	$\frac{23}{2}^+$	$\frac{21}{2}^-$	32.2±14
$^{167}_{69}Tm_{98}$	172	$[411\ \frac{1}{2}]\rightarrow[541\ \frac{1}{2}]$	85.1	$\frac{11}{2}^+$	$\frac{9}{2}^-$	11.2±1
			99.2	$\frac{11}{2}^+$	$\frac{13}{2}^-$	11.7±1.2*
			385.5	$\frac{13}{2}^+$	$\frac{15}{2}^-$	12.3±1.3*
			218.9	$\frac{15}{2}^+$	$\frac{13}{2}^-$	9.6±0.6
			387.3	$\frac{17}{2}^+$	$\frac{19}{2}^-$	12.9±5*
			345.2	$\frac{19}{2}^+$	$\frac{17}{2}^-$	8.4±0.6
$^{169}_{71}Lu_{98}$	68	$[411\ \frac{1}{2}]\rightarrow[541\ \frac{1}{2}]$	218.0	$\frac{7}{2}^+$	$\frac{5}{2}^-$	≤0.04
			368.0	$\frac{11}{2}^+$	$\frac{9}{2}^-$	≤0.046
			512.5	$\frac{15}{2}^+$	$\frac{13}{2}^-$	0.31±0.07
			635.0	$\frac{19}{2}^+$	$\frac{17}{2}^-$	0.11±0.04
			720.8	$\frac{23}{2}^+$	$\frac{21}{2}^-$	1.23±0.20
			773.1	$\frac{27}{2}^+$	$\frac{25}{2}^-$	2.86±0.35
			803.2	$\frac{31}{2}^+$	$\frac{29}{2}^-$	3.30±0.45
			822.4	$\frac{35}{2}^+$	$\frac{33}{2}^-$	2.75±0.75
	439	$[514\ \frac{9}{2}]\rightarrow[404\ \frac{7}{2}]$	412.7	$\frac{13}{2}^-$	$\frac{11}{2}^+$	0.44±0.15
			244.1	$\frac{13}{2}^-$	$\frac{13}{2}^+$	4.6±0.9
			405.4	$\frac{15}{2}^-$	$\frac{13}{2}^+$	1.1±0.2
			403.0	$\frac{17}{2}^-$	$\frac{15}{2}^+$	1.9±0.3
			397.0	$\frac{19}{2}^-$	$\frac{17}{2}^+$	1.1±0.3
$^{171}_{71}Lu_{100}$	137	$[411\ \frac{1}{2}]\rightarrow[541\ \frac{1}{2}]$	292.0	$\frac{7}{2}^+$	$\frac{5}{2}^-$	0.04±0.02
			453.1	$\frac{11}{2}^+$	$\frac{9}{2}^-$	0.20±0.07
			615.3	$\frac{15}{2}^+$	$\frac{13}{2}^-$	0.30±0.08
			760.3	$\frac{19}{2}^+$	$\frac{17}{2}^-$	2.4±0.6
$^{173}_{71}Lu_{102}$	297	$[411\ \frac{1}{2}]\rightarrow[541\ \frac{1}{2}]$	289.0	$\frac{5}{2}^+$	$\frac{3}{2}^-$	1.08±0.43
			349.8	$\frac{9}{2}^+$	$\frac{7}{2}^-$	1.63±0.65
			621.6	$\frac{11}{2}^+$	$\frac{9}{2}^-$	0.49±0.15
			461.7	$\frac{11}{2}^+$	$\frac{13}{2}^-$	0.95±0.29
			795.9	$\frac{15}{2}^+$	$\frac{13}{2}^-$	2.18±0.87
$^{157}_{67}Ho_{90}$	67	$[404\ \frac{7}{2}]\rightarrow[523\ \frac{7}{2}]$	324.6	$\frac{11}{2}^+$	$\frac{7}{2}^-$	1.25±0.20
			422.0	$\frac{13}{2}^+$	$\frac{11}{2}^-$	1.50±0.14
			477.0	$\frac{15}{2}^+$	$\frac{13}{2}^-$	2.40±0.26
			566.6	$\frac{17}{2}^+$	$\frac{15}{2}^-$	0.82±0.07
			578.5	$\frac{19}{2}^+$	$\frac{17}{2}^-$	0.85±0.12
			665.2	$\frac{21}{2}^+$	$\frac{19}{2}^-$	1.54±0.12
			638.3	$\frac{23}{2}^+$	$\frac{21}{2}^-$	1.37±0.18
			719.4	$\frac{25}{2}^+$	$\frac{23}{2}^-$	1.61±0.14
			(654.6	$\frac{27}{2}^+$	$\frac{25}{2}^-$	1.70±0.19)

TABLE IV. Continued.

Nucleus	Δe (keV)	$[Nn_z\Lambda\Omega]^{(i)}\rightarrow$ $[Nn_z\Lambda\Omega]^{(f)}$	E_γ (keV)	$I^{(i)}$	$I^{(f)}$	$B(E1)$ $(10^{-4}e^2\,\mathrm{fm}^2)$
			Odd neutron			
$^{177}_{72}Hf_{105}$	321	$[624\ \frac{9}{2}]\rightarrow[514\ \frac{7}{2}]$	321.3	$\frac{9}{2}^+$	$\frac{7}{2}^-$	0.0036
			208.3	$\frac{9}{2}^+$	$\frac{9}{2}^-$	0.69
			71.7	$\frac{9}{2}^+$	$\frac{11}{2}^-$	0.23
			313.7	$\frac{11}{2}^+$	$\frac{9}{2}^-$	0.07
			177.0	$\frac{11}{2}^+$	$\frac{11}{2}^-$	1.00
			305.5	$\frac{13}{2}^+$	$\frac{11}{2}^-$	0.24
			145.8	$\frac{13}{2}^+$	$\frac{13}{2}^-$	1.30
			299.0	$\frac{15}{2}^+$	$\frac{13}{2}^-$	0.44
			117.2	$\frac{15}{2}^+$	$\frac{15}{2}^-$	0.98
			291.4	$\frac{17}{2}^+$	$\frac{15}{2}^-$	0.84
			88.4	$\frac{17}{2}^+$	$\frac{17}{2}^-$	1.30
			292.5	$\frac{19}{2}^+$	$\frac{17}{2}^-$	1.10
			69.2	$\frac{19}{2}^+$	$\frac{19}{2}^-$	0.84
			283.4	$\frac{21}{2}^+$	$\frac{19}{2}^-$	1.40
$^{163}_{68}Er_{95}$	69	$[523\ \frac{5}{2}]\rightarrow[642\ \frac{5}{2}]$	267.4	$\frac{13}{2}^-$	$\frac{11}{2}^+$	1.00±0.10
			394	$\frac{15}{2}^-$	$\frac{13}{2}^+$	1.55±0.55
			409.4	$\frac{17}{2}^-$	$\frac{15}{2}^+$	1.90±0.10
			569.4	$\frac{19}{2}^-$	$\frac{17}{2}^+$	5.00±2.20
			509	$\frac{21}{2}^-$	$\frac{19}{2}^+$	3.40±0.50
			703.0	$\frac{23}{2}^-$	$\frac{21}{2}^+$	4.20±1.90
$^{163}_{70}Yb_{93}$	99	$[521\ \frac{3}{2}]\rightarrow[642\ \frac{5}{2}]$	263.8	$\frac{13}{2}^-$	$\frac{11}{2}^+$	≤ 4.5
			429.4	$\frac{17}{2}^-$	$\frac{15}{2}^+$	1.96±0.6
			504.1	$\frac{21}{2}^-$	$\frac{19}{2}^+$	≤ 2.9
			475.0	$\frac{25}{2}^-$	$\frac{23}{2}^+$	9.1±2.7
$^{165}_{70}Yb_{95}$		$[523\ \frac{5}{2}]\rightarrow[642\ \frac{5}{2}]$	274.6	$\frac{13}{2}^-$	$\frac{11}{2}^+$	0.61±0.18
			431.0	$\frac{17}{2}^-$	$\frac{15}{2}^+$	≤ 0.5
			522.0	$\frac{21}{2}^-$	$\frac{19}{2}^+$	1.90±0.60
			546.8	$\frac{25}{2}^-$	$\frac{23}{2}^+$	≥ 2.2
$^{167}_{70}Yb_{97}$	30	$[523\ \frac{5}{2}]\rightarrow[642\ \frac{5}{2}]$	316.6	$\frac{13}{2}^-$	$\frac{11}{2}^+$	≤ 3.2
			453.0	$\frac{17}{2}^-$	$\frac{15}{2}^+$	2.6±0.78
			548.0	$\frac{21}{2}^-$	$\frac{19}{2}^+$	0.96±0.30
			596.0	$\frac{25}{2}^-$	$\frac{23}{2}^+$	≤ 1.0

thus be estimated in a relatively reliable way.

Since, in the following, we are interested only in the contribution from a particular orbital to the sum in (5), we further approximate the model by estimating b_ν values. Namely, as is illustrated in Fig. 8, we replace the RPA excitation modes "i" in (5), which include the correlation coming from the $\Delta N_t=1$ and $\Delta N_t=2$ excitations and are expressed by wavy lines in Fig. 8, by $\Delta N_t=1$ two-quasiparticle (2qp) excitations "j," which are represented by bubbles. Correspondingly, the bare octupole-octupole interaction should be replaced by a renormalized one, which is indicated by double lines in Fig. 8. The expression of b_ν parameters in (5) for $E1$ transitions in odd-A nuclei is now written as

$$
\begin{aligned}
eb_\nu = &-\sum_{j(2\mathrm{qp})\neq j_i}(\tilde{\kappa}_0+\tilde{\kappa}_1)\left[\frac{1}{E^j_{2\mathrm{qp}}}\right]\langle j,\tau=1|r^3Y^*_{3\nu}|0\rangle\langle 0|\tilde{O}(E1,\nu)|j,\tau=1\rangle \\
&-\sum_{j(2\mathrm{qp})\neq j_f}(\tilde{\kappa}_0+\tilde{\kappa}_1)\left[\frac{1}{E^j_{2\mathrm{qp}}}\right]\langle j,\tau=1|r^3Y^*_{3\nu}|0\rangle\langle 0|\tilde{O}(E1,\nu)|j,\tau=1\rangle \\
&-\sum_{j(2\mathrm{qp})}(\tilde{\kappa}_0-\tilde{\kappa}_1)\left[\frac{2}{E^j_{2\mathrm{qp}}}\right]\langle j,\tau=-1|r^3Y^*_{3\nu}|0\rangle\langle 0|\tilde{O}(E1,\nu)|j,\tau=-1\rangle\ ,
\end{aligned}
\tag{7}
$$

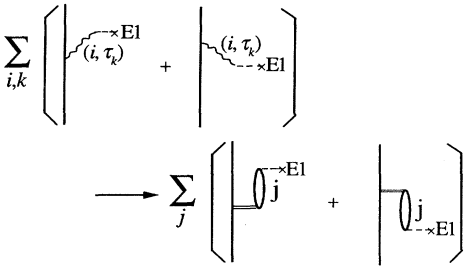

FIG. 8. Illustration of the renormalization of octupole-octupole interaction strength coming from the replacement of summation over all RPA modes by summation over $\Delta N_t=1$ two-quasiparticle (2qp) excitations.

where $\tilde{\kappa}_0$ ($\tilde{\kappa}_1$) are the renormalized isoscalar (isovector) octupole-octupole coupling constants. The blocking effect in the like-particle channel is taken into account in the first two terms of Eq. (7), namely, all the two-quasiparticle excitations $j_i(j_f)$ involving the one-quasiparticle orbital in the initial (final) state of the $E1$ transition in odd-A nuclei are removed from the summation. In this estimate of the blocking effect, the approximation was made in which only the rotationally unperturbed component of the initial and the final wave function in odd-A nuclei was blocked. Since the sum in (7) is taken over all $\Delta N_t=1$ 2qp excitations (namely, all configurations producing the giant dipole resonance are included), in the expression (1) of the $E1$ effective charge the polarizability χ is set equal to zero.

In Fig. 9 we show calculated contributions (apart from the renormalized coupling constant) to the expression (7) as a function of 2qp energy, taking as an example the nucleus ^{169}Lu for which ^{168}Yb is the core. It is seen that for a given ν there is a cancellation within the neutron (or proton) 2qp contributions and, moreover, the total contribution from neutrons has an opposite sign to the total contribution from protons. We further note that the contributions from all lower-lying 2qp excitations are small but have a definite sign (for a given kind of particle) and that only a limited number of higher-lying 2qp configurations (with specific combinations of asymptotic quantum numbers) contribute significantly. When we denote the asymptotic quantum numbers of the 2qp orbitals by $[Nn_z\Lambda\Omega]$ and $[N'n_z'\Lambda'\Omega']$, respectively, among those higher-lying 2qp configurations we observe that (a) the positive (negative) contributions in the lower part of Fig. 9 (namely, the $\nu=1$ component) for neutrons (protons) come exclusively from the 2qp orbitals with $n_z=n_z'=0$; and (b) similarly, the positive (negative) contributions in the upper part of Fig. 9 (namely, the $\nu=0$ component) for neutrons (protons) come from the pairs in which one of the 2qp orbitals has $n_z=0$, while the other one has $n_z=1$.

By open symbols in the rhs part (i.e., for protons) of Fig. 9 we indicate the contributions in which either the $[541\ \frac{1}{2}]$ or the $[411\ \frac{1}{2}]$ orbitals are involved. That means those contributions are excluded in the sum (7) calculated for $E1$ transitions between the $[541\ \frac{1}{2}]$ and the $[411\ \frac{1}{2}]$ band, corresponding to the blocking effect in either the initial or the final state of the odd-A nucleus. From Fig. 9 it is clearly seen that the largest value (coming from the $[541\ \frac{1}{2}]$ $[431\ \frac{1}{2}]$ 2qp configuration) among the open circles in the upper right part of the figure may be comparable with the final value of the $\nu=0$ sum, which comes out from a cancellation of the contributions from neutrons and protons.

Assuming that the difference of the b_0 (or b_1) values for the two sets of observed $E1$ transitions, (A) between the $[541\ \frac{1}{2}]$ and the $[411\ \frac{1}{2}]$ band and (B) between the $[514\ \frac{9}{2}]$ and the $[404\ \frac{7}{2}]$ band, in ^{169}Lu comes entirely from the difference in blocking effects, we make a theoretical estimate of the difference $b_\nu^{(A)}-b_\nu^{(B)}$. Following the renormalization procedure given in Ref. [1] we obtain the isoscalar and the isovector renormalized coupling constants

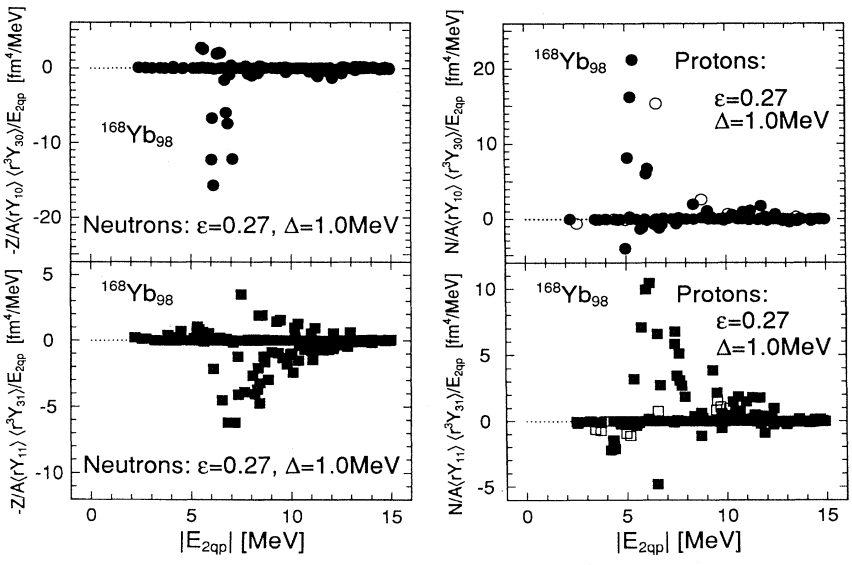

FIG. 9. Calculated contributions to the expression (7) (apart from the renormalized coupling constants) for ^{169}Lu as a function of two-quasiparticle (2qp) energies. Open symbols express blocked contributions for the transition between $[411\ \frac{1}{2}]$ and the $[541\ \frac{1}{2}]$ band. See text for details.

for $A=170$ as

$$\tilde{\kappa}_0 \approx 3\kappa_0 = 3(-1.6\times10^{-5})\ \text{MeV fm}^{-6}\ ,$$
$$\tilde{\kappa}_1 \approx 0.2\kappa_1 = 0.2(+7.9\times10^{-5})\ \text{MeV fm}^{-6}\ . \tag{8}$$

Though the values of the renormalized coupling constants depend on the energy difference between the important RPA modes and the relevant 2qp excitations, in the present estimate we have used the values in the static limit, namely, in the limit where the frequencies of all important RPA modes are much larger than the relevant 2qp excitations.[1] Using the values in Eq. (8), we obtain

$$\begin{aligned}\Delta b_0^{\text{theo}} &\equiv [b_0^{(\text{A})}]_{\text{theo}} - [b_0^{(\text{B})}]_{\text{theo}} \\ &= [\delta b_0^{(\text{A})}]_{\text{theo}} - [\delta b_0^{(\text{B})}]_{\text{theo}} \\ &\approx -0.0013\ \text{fm}^{-2}\ , \\ \Delta b_1^{\text{theo}} &\equiv [b_0^{(\text{A})}]_{\text{theo}} - [b_0^{(\text{B})}]_{\text{theo}} \\ &= [\delta b_1^{(\text{A})}]_{\text{theo}} - [\delta b_1^{(\text{B})}]_{\text{theo}} \\ &\approx -0.0000\ \text{fm}^{-2}\ ,\end{aligned} \tag{9}$$

where δb_ν expresses the blocking contribution. We note the difference of b_ν values obtained from the analysis of experimental data (see Table III):

$$\begin{aligned}\Delta b_0^{\text{exp}} &\equiv [b_0^{(\text{A})}]_{\text{exp}} - [b_0^{(\text{B})}]_{\text{exp}} \approx -0.014\ \text{fm}^{-2}\ , \\ \Delta b_1^{\text{exp}} &\equiv [b_1^{(\text{A})}]_{\text{exp}} - [b_1^{(\text{B})}]_{\text{exp}} \approx -0.003\ \text{fm}^{-2}\ .\end{aligned} \tag{10}$$

From the comparison of the results given by (9) and (10) we see that the sign of Δb_0^{theo} is the same as that of Δb_0^{exp} and that the obtained relation $|\Delta b_0^{\text{theo}}| \gg |\Delta b_1^{\text{theo}}|$ is in agreement with $|\Delta b_0^{\text{exp}}| \gg |\Delta b_1^{\text{exp}}|$. However, the estimated magnitude of Δb_0^{theo} is an order of magnitude smaller than Δb_0^{exp}. Even when we take into account various ambiguities involved in the present analysis, the difference of a factor of 10 seems to be a bit surprising and is presently difficult to understand.[2]

IV. SUMMARY

Using a model in which one quasiparticle is coupled to an axially symmetric rotor, we have analyzed $E1$ transition strengths observed at angular momenta lower than that of the S-band crossing in the yrast spectroscopy of odd-A rare-earth nuclei. After varying adjustable parameters in the model within acceptable ranges so as to reproduce satisfactorily the characteristic features of the observed level scheme of each nucleus, the $E1$ strengths are calculated by using the resulting wave functions. It has been found that the $B(E1)$ values estimated in the model are too small (at least by an order of magnitude) compared with observed ones when reasonable values of the $E1$ effective charge are used.

Since there is no other obvious element which may lead to an enhancement of $E1$ strengths by more than an order of magnitude, we invoke a contribution from possible octupole softness to the $E1$ strengths, though those rare-earth nuclei discussed in the present work are usually supposed to be fully stable against octupole deformation. We have analyzed available experimental $B(E1)$ values in terms of b_ν parameters, which effectively express the effect of octupole vibrations on the $E1$ transitions. We have found that the b_ν values necessary for reproducing experimental $B(E1)$ values are of the order of 10^{-2} fm^{-2} and that the b_ν values depend on nuclei and are sensitive to selected pairs of bands. Considering the fact that a special high accuracy which may certainly go beyond the accuracy of any presently available microscopic models is needed for making a reliable quantitative estimate of the absolute magnitudes of the b_ν values, in the present paper we give up on calculating the absolute magnitudes of b_ν parameters which should be compared with the b_ν parameters obtained from the analysis of experimental $B(E1)$ values. Instead, taking the two sets of $E1$ transitions observed in the same nucleus ^{169}Lu (namely, the $E1$ transitions between the [541 $\frac{1}{2}$] and the [411 $\frac{1}{2}$] band, and those between the [514 $\frac{9}{2}$] and the [404 $\frac{7}{2}$] band), we have compared the difference of the b_0 (and b_1) parameters obtained from the analysis of experimental $B(E1)$ values with that from our microscopic estimate. The difference is supposed to come from the blocking effect due to the presence of the odd particle occupying particular orbitals. A contribution from a particular orbital to b_ν parameters is expected to be estimated with a higher accuracy than that of the total magnitudes of b_ν parameters, which are the consequence of many subtle cancellations.

The comparison between the difference of the b_0 (and b_1) parameters shows that the sign of Δb_0 as well as the relation $|\Delta b_0| \gg |\Delta b_1|$ is correctly obtained. However, the absolute magnitude of Δb_0 obtained in our microscopic estimate is an order of magnitude smaller than that obtained from the analysis of experimental $B(E1)$ values. Such a large difference is at present difficult to understand, even when we take into account various ambiguities involved in our present microscopic calculations as well as in our analysis of experimental information. However, we notice that, in the shell-correction calculations [8] of the dipole moments in the Ba-Sm and the Ra-Th region, the agreement of calculated moments with experimental information depends on the adopted value of the macroscopic constants in the droplet model. And, the adopted values are, to some extent, adjusted parameters.

ACKNOWLEDGMENTS

The authors would like to thank Dr. X. Z. Zhang for the computer programs which are partially used in the

[1] Since the 2q configurations, which make the major contributions to the blocking effect on the b_ν parameters, lie around the energy of $1\hbar\omega_0$ excitations, to use the values in the static limit is a rough approximation.

[2] We performed also a similar analysis using double-stretched octupole-octupole interaction [22]. The results and conclusions appear to be comparable with those described in the text.

analysis presented in Sec. III A. We are also indebted to Dr. P. Butler for an informative communication of experimental data and to Dr. S. Mizutori for many stimulating discussions concerning the microscopic evaluation of b_ν parameters. One of us (W.S.) acknowledges the financial support of the Department of Mathematical Physics and Lund University of Technology founded by the Swedish Natural Science Research Council (NFR).

[1] A. Bohr and B. R. Mottelson, *Nuclear Structure* (Benjamin, New York, 1975), Vol. 2.
[2] V. M. Strutinsky, J. Nucl. Energy **4**, 523 (1957).
[3] A. Bohr and B. R. Mottelson, Nucl. Phys. **4**, 529 (1957); **9**, 687 (1958/59).
[4] F. S. Stephens, F. Asaro, and I. Perlman, Phys. Rev. **100**, 1543 (1955).
[5] P. Möller, S. G. Nilsson, and R. K. Sheline, Phys. Lett. **40B**, 329 (1972).
[6] R. R. Chasman, Phys. Lett. **96B**, 7 (1980).
[7] G. A. Leander, W. Nazarewicz, G. F. Bertsch, and J. Dudek, Nucl. Phys. **A453**, 58 (1986).
[8] P. A. Butler and W. Nazarewicz, Nucl. Phys. **A533**, 249 (1991).
[9] J. L. Egido and L. M. Robledo, Nucl. Phys. **A494**, 85 (1989).
[10] K. Neergaard and P. Vogel, Nucl. Phys. **A145**, 33 (1970); **A149**, 209, 217 (1970).
[11] I. Hamamoto, J. Höller, and X. Z. Zhang, Phys. Lett. B **226**, 17 (1989).
[12] M. N. Vergnes and J. O. Rasmussen, Nucl. Phys. **62**, 233 (1965).
[13] A. Faessler, T. Udagawa, and R. K. Sheline, Nucl. Phys. **85**, 670 (1966).
[14] F. M. Bernthal and J. O. Rasmussen, Nucl. Phys. **A101**, 513 (1967).
[15] P. Alexander, F. Boehm, and E. Kankeleit, Phys. Rev. **133**, B284 (1964); A. J. Haverfield, F. M. Bernthal, and J. M. Hollander, Nucl. Phys. **A94**, 337 (1967).
[16] Yu. T. Grin and I. M. Pavlichenkow, Phys. Lett. **9**, 249 (1964).
[17] I. Hamamoto and H. Sagawa, Nucl. Phys. **A327**, 99 (1979).
[18] S. Ogaza, J. Kownacki, H. Jensen, J. Gascon, G. B. Hagemann, Y. Iwata, T. Komatsubara, G. Sletten, P. O. Tjøm, W. Waluś, and I. Hamamoto, Nucl. Phys. A (in press).
[19] I. Hamamoto and H. Sagawa, Phys. Lett. **85B**, 177 (1979).
[20] A. H. Wapstra and G. Audi, Nucl. Phys. **A432**, 55 (1985).
[21] I. Hamamoto, Nucl. Phys. **A205**, 225 (1973).
[22] H. Sakamoto and T. Kishimoto, Nucl. Phys. **A501**, 205 (1989).
[23] J. Gizon, A. Gizon, S. A. Hjorth, D. Barneoud, S. Andre, and J. Treherne, Nucl. Phys. **A193**, 193 (1972); Nucl. Data Sheets **50**, 137 (1987).
[24] S. Olbrich, V. Ionescu, J. Kern, C. Nordmann, and W. Reichert, Nucl. Phys. **A342**, 133 (1980).
[25] P. Kemnitz, L. Funke, K.-H. Kaun, H. Sodan, G. Winter, and M. I. Baznat, Nucl. Phys. **A209**, 271 (1973).
[26] A. Brockstedt, J. Lyttkeus-Lindén, M. Bergström, L. P. Ekström, H. Ryde, J. C. Bacelar, J. D. Garrett, G. B. Hagemann, B. Herskind, F. R. May, P. O. Tjøm, and S. Frauendorf (unpublished).
[27] J. Kownacki, J. D. Garrett, J. J. Gaardhøje, G. B. Hagemann, B. Herskind, S. Jónsson, N. Roy, H. Ryde, and W. Waluś, Nucl. Phys. **A394**, 269 (1983).
[28] N. Roy, S. Jónsson, H. Ryde, W. Waluś, J. j. Gaardhøje, J. D. Garrett, G. B. Hagemann, and B. Herskind, Nucl. Phys. **A382**, 125 (1982).
[29] D. C. Radford, H. R. Andrews, G. C. Ball, D. Horn, D. Ward, F. Banville, S. Flibotte, S. Monaro, S. Pilotte, P. Taras, J. K. Johansson, D. Tucker, J. C. Waddington, M. A. Riley, G. B. Hagemann, and I. Hamamoto, Nucl. Phys. **A545**, 665 (1992).
[30] G. B. Hagemann, B. Herskind, J. Kownacki, B. M. Nyakó, P. J. Nolan, J. F. Sharpey-Schafer, and P. O. Tjøm, Nucl. Phys. **A424**, 365 (1984).